

Stoilov I, Akarsu AN, Sarfarazi M (1997) Identification of three different truncating mutations in cytochrome P4501B1 (CYP1B1) as the principal cause of primary congenital glaucoma (Buphthalmos) in families linked to the GLC3A locus on chromosome 2p21. *Hum Mol Genet* 6:641-7.

Stone EM, Fingert JH, Alward WL, Nguyen TD, Polansky JR, Sunden SL, Nishimura D, Clark AF, Nystuen A, Nichols BE, Mackey DA, Ritch R, Kalenak JW, Craven ER, Sheffield VC (1997) Identification of a gene that causes primary open angle glaucoma. *Science* 275:668-70.

Tan O, Li G, Lu AT, Varma R, Huang D; Advanced Imaging for Glaucoma Study Group (2008) Mapping of macular substructures with optical coherence tomography for glaucoma diagnosis. *Ophthalmology* 115:949-56.

Wang L, Cioffi GA, Cull G, Dong J, Fortune B (2002) Immunohistologic evidence for retinal glial cell changes in human glaucoma. *Invest Ophthalmol Vis Sci* 43:1088-94.

Wässle H, Grünert U, Röhrenbeck J, Boycott BB (1989) Cortical magnification factor and the ganglion cell density of the primate retina. *Nature* 341:643-6.

Watanabe T, Raff MC (1988) Retinal astrocytes are immigrants from the optic nerve. *Nature* 332:834-7.

Willoughby CE, Chan LL, Herd S, Billingsley G, Noordeh N, Levin AV, Buys Y, Trope G, Sarfarazi M, Heon E (2004) Defining the pathogenicity of optineurin in juvenile open-angle glaucoma. *Invest Ophthalmol Vis Sci* 45:3122-3130.

Zerial M, McBride H (2001) Rab proteins as membrane organizers. *Nat Rev Mol Cell Biol* 2:107-117.

FIGURE LEGENDS

Figure 1.

Development of transgenic mouse over expressing OPTN.

A, Schematic diagram of the OPTN constructs used in this study. The green region corresponds to the OPTN protein. Positions of mutations and deletions are shown in red. The HA tag is marked by yellow color. The CAGGS region corresponds to the

chicken beta-actin promoter. **B**, Fundus photographs of normal, Wt and E50K Tg mouse eyes at 16 month. Curvature of the retinal vessels indicates the excavation of the area including the optic disc in E50K Tg mouse eye. **C**, Total expression of endogenous and mutant OPTN (red) in the retina of normal and E50K Tg mice at 16 month. Anti-OPTN antibody and Anti-HA antibody were used to detect endogenous and mutant OPTN respectively. Scale bar, 50 μm .

Figure 2.

RGC loss and thinning of the retina thickness in the peripheral retina.

A, staining of retina sections of 16 month old normal and Tg mice. Scale bar, 200 μm (upper panel), 50 μm (lower panel). **B**, Quantification of the RGC number and retina thickness of 16 month old normal and Tg mice (n=6). Only 50K Tg mice at 16 months showed significant RGC loss and thinning of retina (** $p < 0.01$). **C**, Quantification of the RGC number and retina thickness during development of E50K Tg mice (n=6). Tg mice showed statistically significant RGC loss and thinning of the retina starting from 12 months of age. **D**, Impaired ERG in E50K Tg mice. The amplitude of the PhNR by E50K Tg mice decreased and removed the negative wave to the transient b-wave (arrow), suggesting RGC loss and other abnormality.

Figure 3.

Histopathology of retina and optic nerve of 16 month old Wt and E50K Tg mouse eyes.

A, Immunolabeling of the retina sections with calretinin, a specific marker for RGCs and amacrine cells. Synapse disruption was observed in the E50K Tg mouse retina (arrow). Scale bar, 20 μm . **B**, Hematoxylin-eosin staining and immunostaining with antibodies against tubulin β III isoform in the optic nerve region. Significant thinning of the nerve fiber layer and the excavation of optic disc (arrow) was observed in E50K Tg mice. Scale bar, 100 μm .

Figure 4.

RGC degeneration in E50K Tg mice.

A, Immunostaining of normal, Wt, and E50K Tg mouse whole retinas with antibodies against SMI32, a specific marker of large type RGCs. Scale bar, 500 μm . White box indicate the location of photographs in lane B. **B**, Thinning of NFL, RGC loss. Scale bar, 50 μm . **C**, RGC axon abnormality (arrows) was also observed. Scale bar, 50 μm .

Figure 5.

Glia cells death in E50K Tg mice.

A, B, Flat mount retina of *E50K* Tg mice was double immunostained with SMI32 (red) and active caspase-3 (green) antibodies. Apoptotic cells were observed only in the whole mount retina of *E50K* Tg mice. Scale bar, 100 μ m. **C-E**, Flat mount retina of *E50K* Tg mice was also double immunostained with active caspase-3 (green) and GFAP (red) antibodies showing apoptosis of astrocytes. Scale bar, 50 μ m. **F**, Apoptotic astrocytes (green) in peripheral retina. **G**, Apoptotic astrocytes (green) in central retina. Scale bar, 100 μ m.

Figure 6

IOP measurements for Wt and E50K Tg mice.

A, impact-rebound tonometer and **B**, optical interferometry tonometer. Both methods gave normal IOP of 15 +/-1 mmHg for Tg mice at all ages examined (n=6).

Figure 7

Disruption of OPTN-Rab8 interaction by E50K mutation.

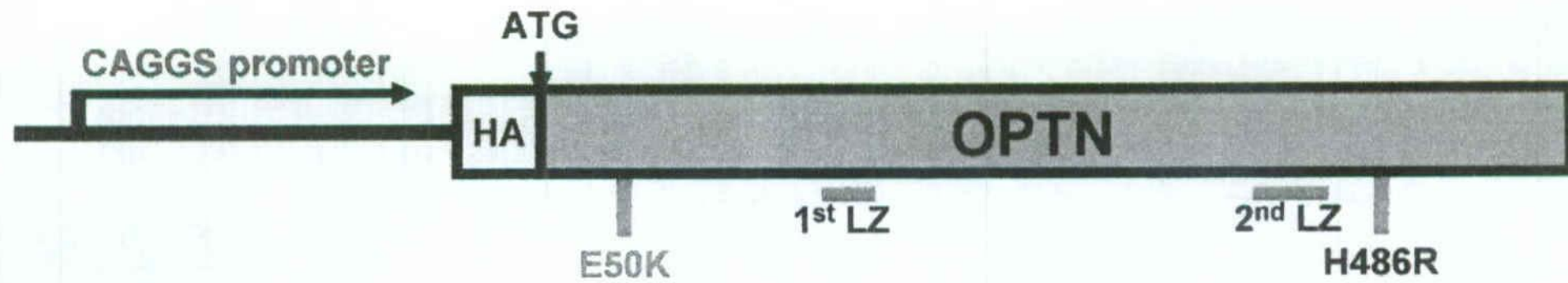
A, A diagram of cDNA constructs used in experiments to study protein-protein interaction. **B**, The protein-protein interaction of OPTN Wt and E50K with Rab8 Wt, T22N inactive form, and Q67L active form as measured in RGC-5 cells. Interaction of OPTN Wt and Q67L active form of Rab8 increased two and five times over Rab8 Wt

or T22N inactive form of Rab8 protein, respectively (** $p < 0.01$). OPTN E50K did not show any interaction with any construct including the active form of Rab8 (n=6). **C**, Protein interaction of Wt or mutant OPTN E50K with Rab8 was measured by QCM technique. A sharp drop of QCM frequency was observed when control OPTN Wt was injected as guest sample, confirming the previous reports of OPTN-Rab8 interaction. Mutant OPTN E50K showed no interaction with Rab8. **D**, GST Pull-down assay to determine OPTN E50K-Rab8 interaction. The fusion protein GST-Rab8 was used for *in vitro* binding assay with purified OPTN Wt and OPTN E50K protein. For negative control OPTN Wt and OPTN E50K were reacted with GST alone (lane 1 & 2). *In vitro* translated OPTN Wt and OPTN E50K were analyzed by SDS-PAGE to show the protein size (lane 6 & 7). OPTN E50K showed significant loss of interaction with Rab8 compare with OPTN Wt (lane 3 & 4, graph). The illustration shows a diagram of the interaction experiment. **E**, Immunostaining the OPTN-Rab8 complex (green) with Golgi marker GM130 (red), indicate that these interactions take place adjacent to the Golgi network.

Figure 8.

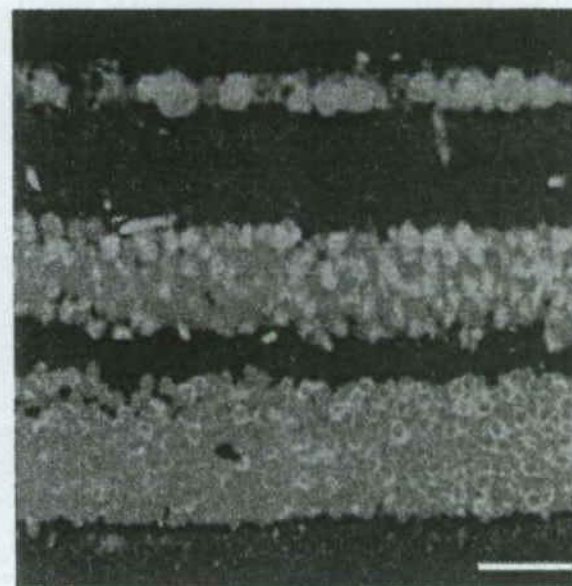
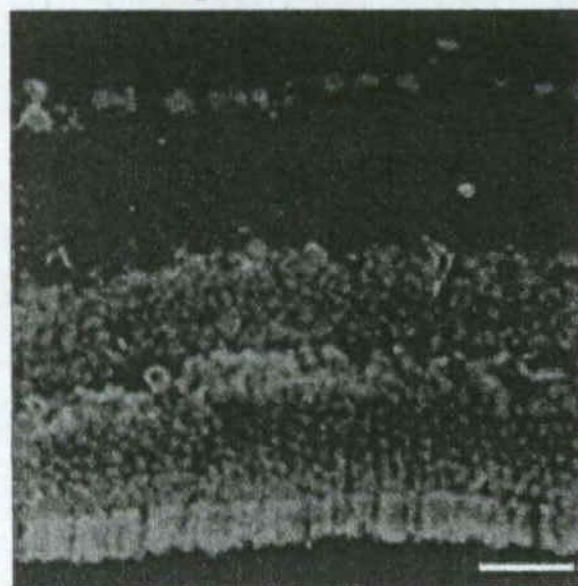
NTG patient with OPTN E50K mutation.

A, A pedigree of a NTG family with OPTN E50K mutation. The patients were diagnosed as NTG with glaucomatous optic neuropathy and visual field loss. **B**, Optical coherence tomography (Cirrus HD-OCT, Carl Zeiss Meditec, Dublin , CA) and visual field test (Humphrey Field Analyzer, Carl Zeiss Medic, Dublin, CA) were shown on patient 2 and unrelated normal control. The retinal NFL thinning and glaucomatous visual field loss were observed in patients.

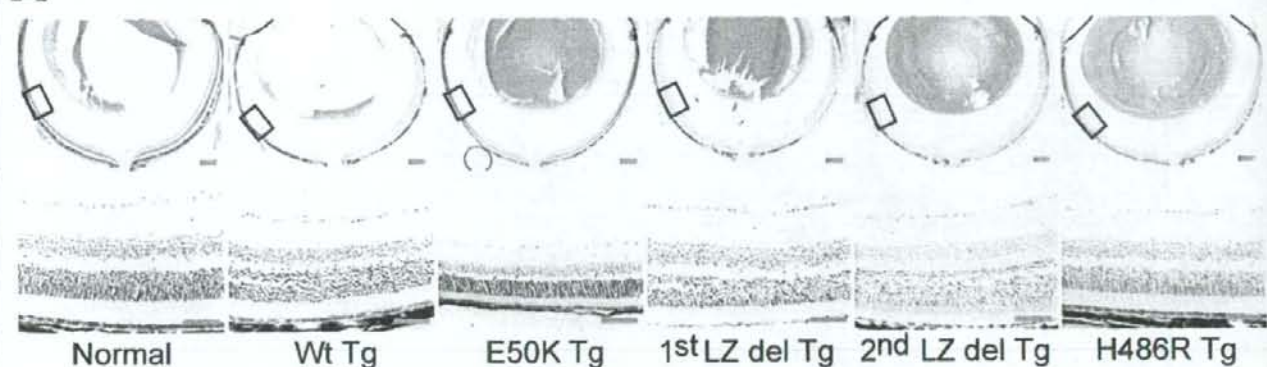
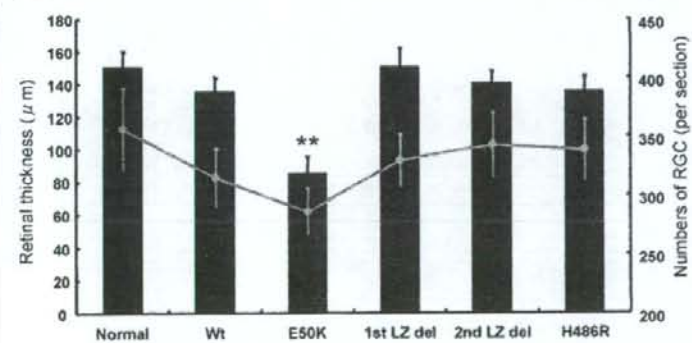
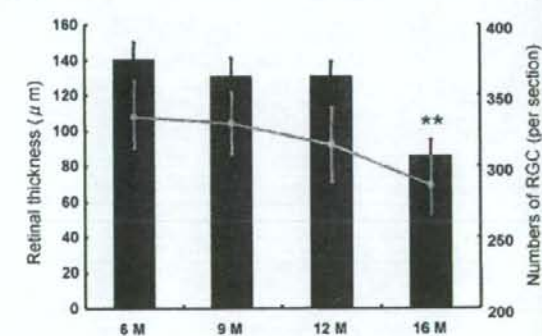
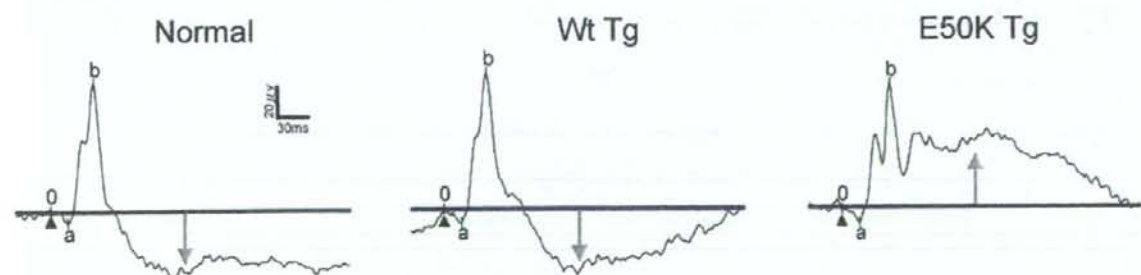
A**B****C**

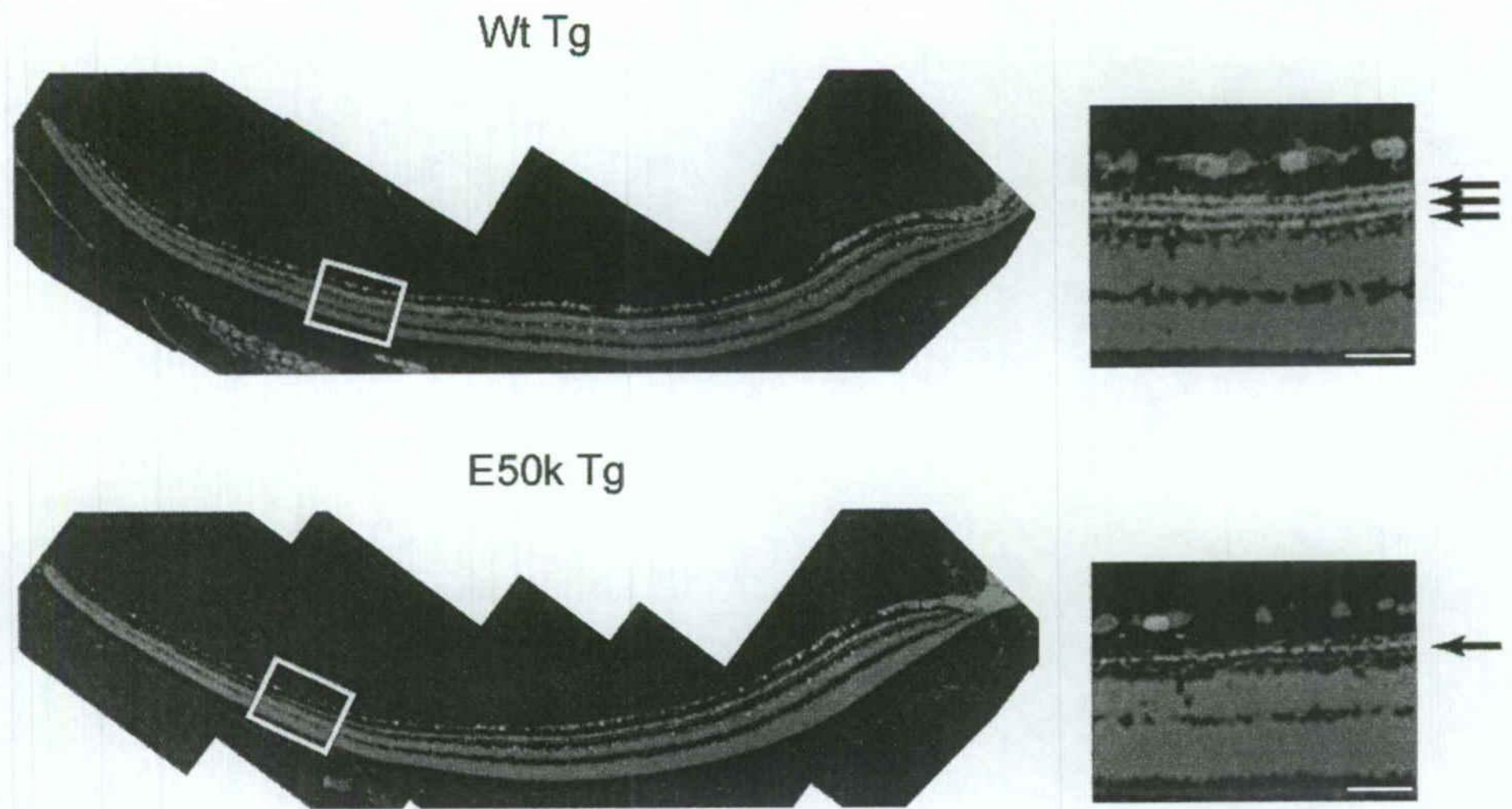
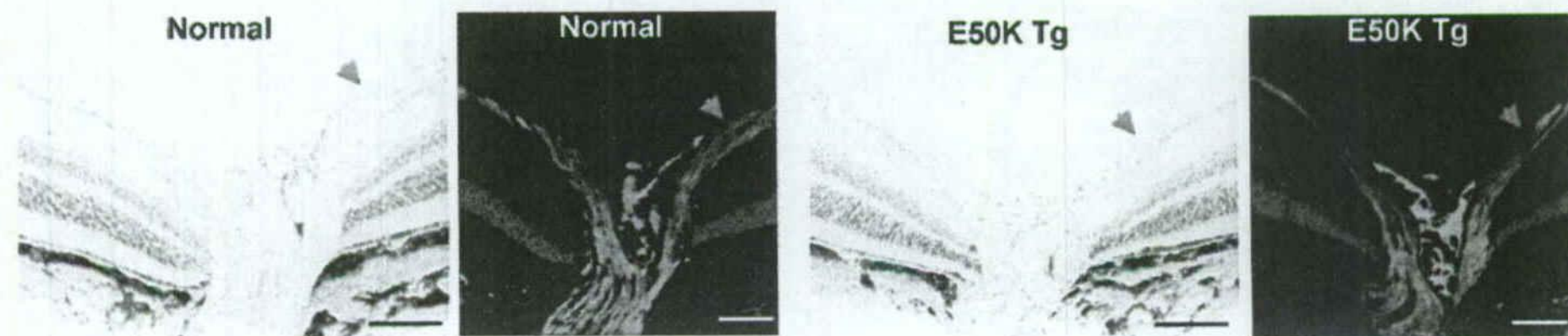
Endogenous OPTN

Mutant OPTN



Ganglion cell layer
 Inner plexiform layer
 Inner nuclear layer
 Outer plexiform layer
 Outer nuclear layer
 Segments of rods and cones

A**B****C****D**

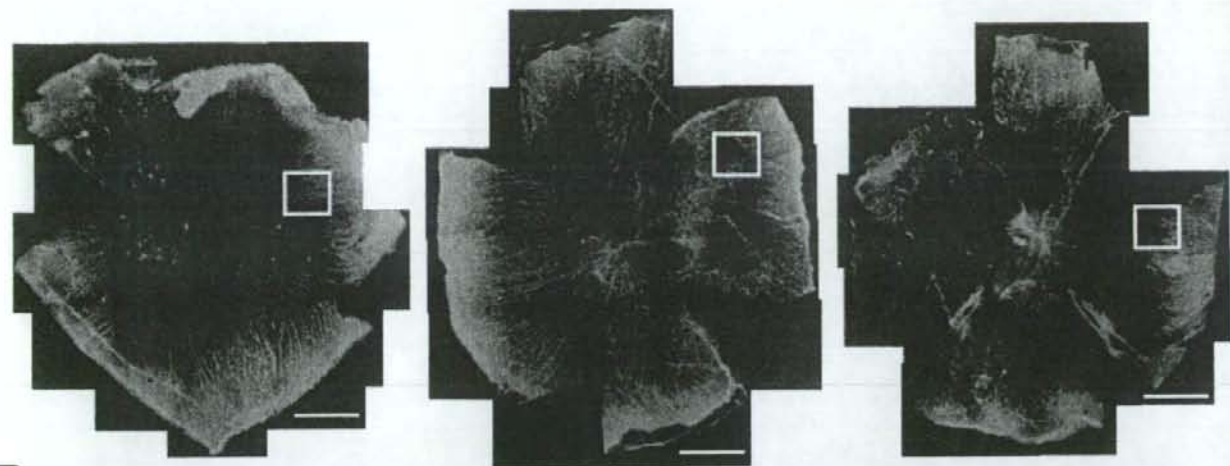
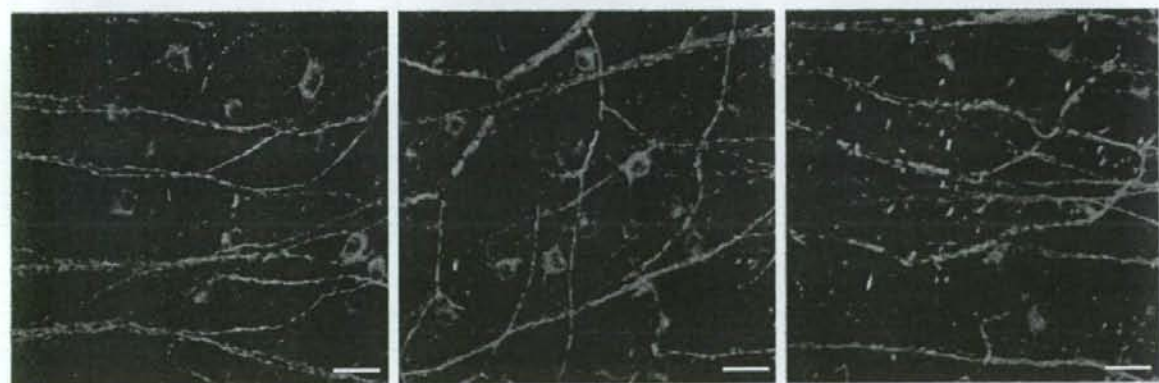
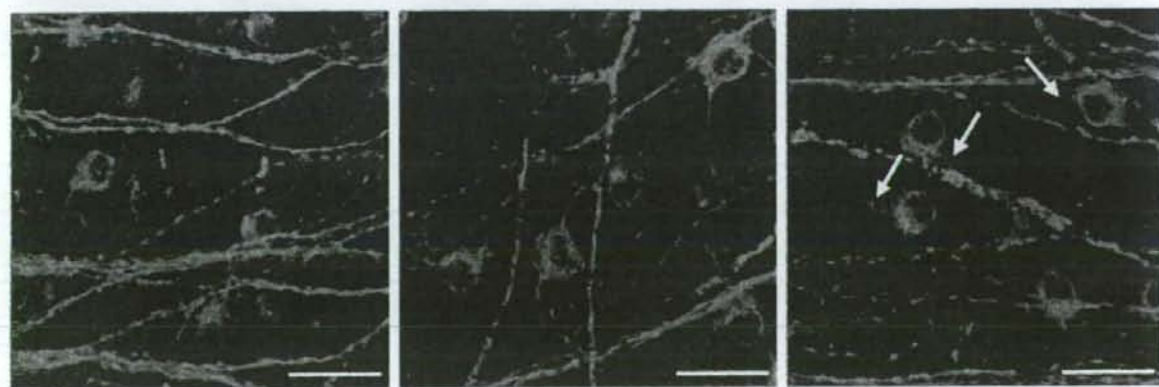
A**B**

A

normal

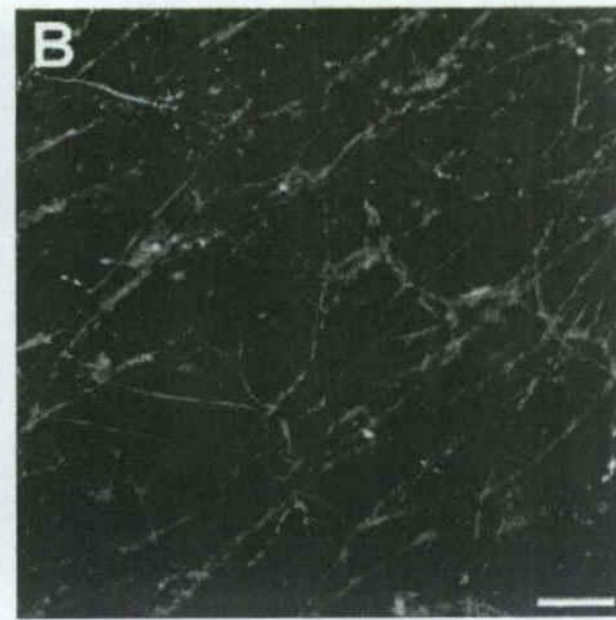
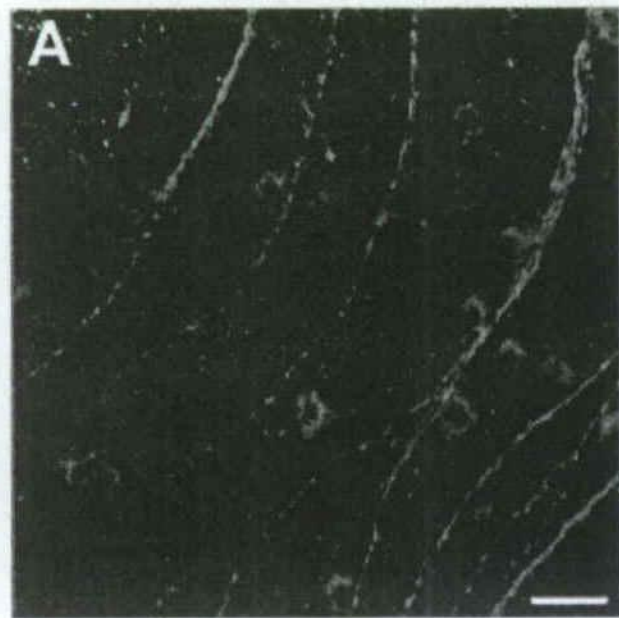
Wt Tg

E50K Tg

**B****C**

Wt Tg

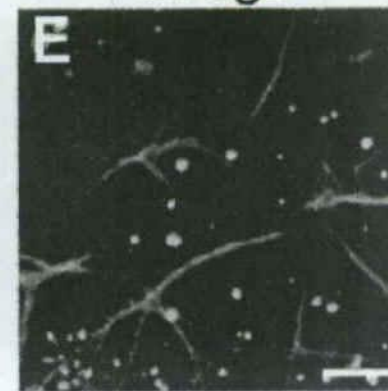
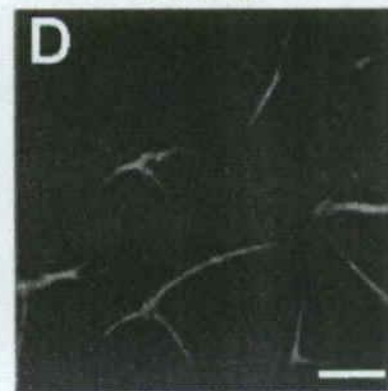
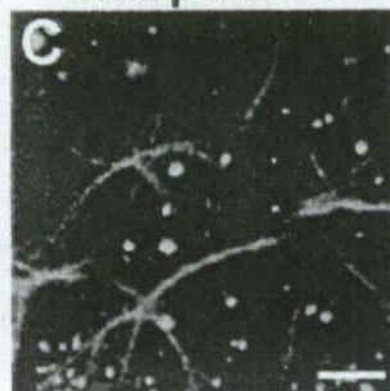
E50K Tg



Caspase-3

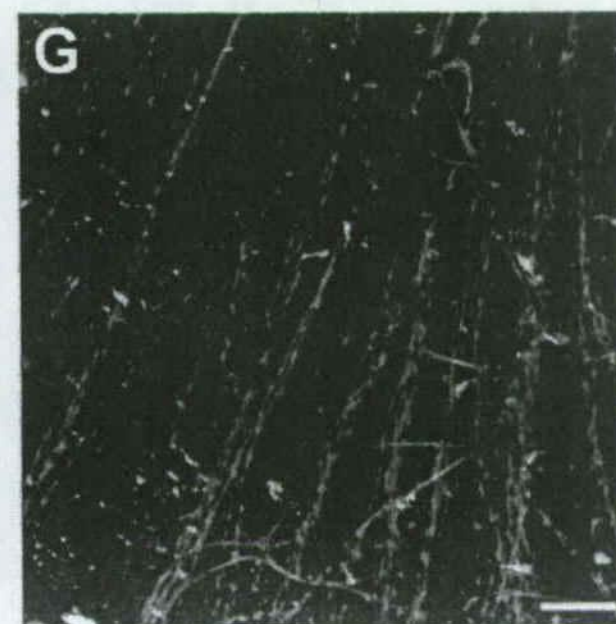
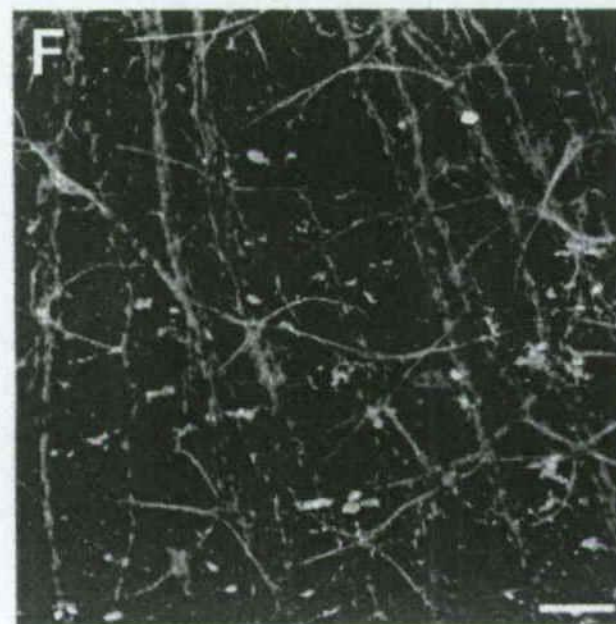
GFAP

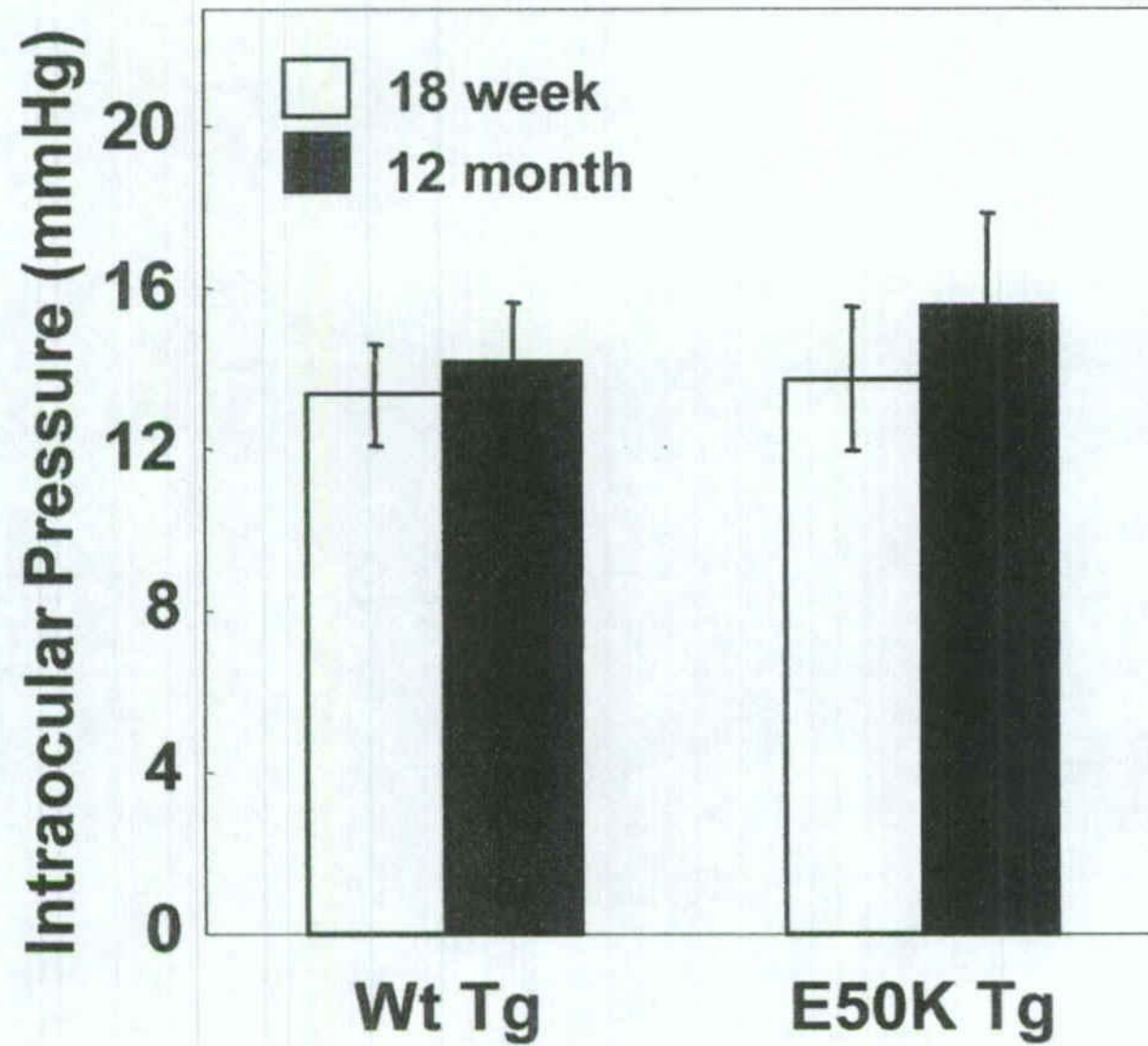
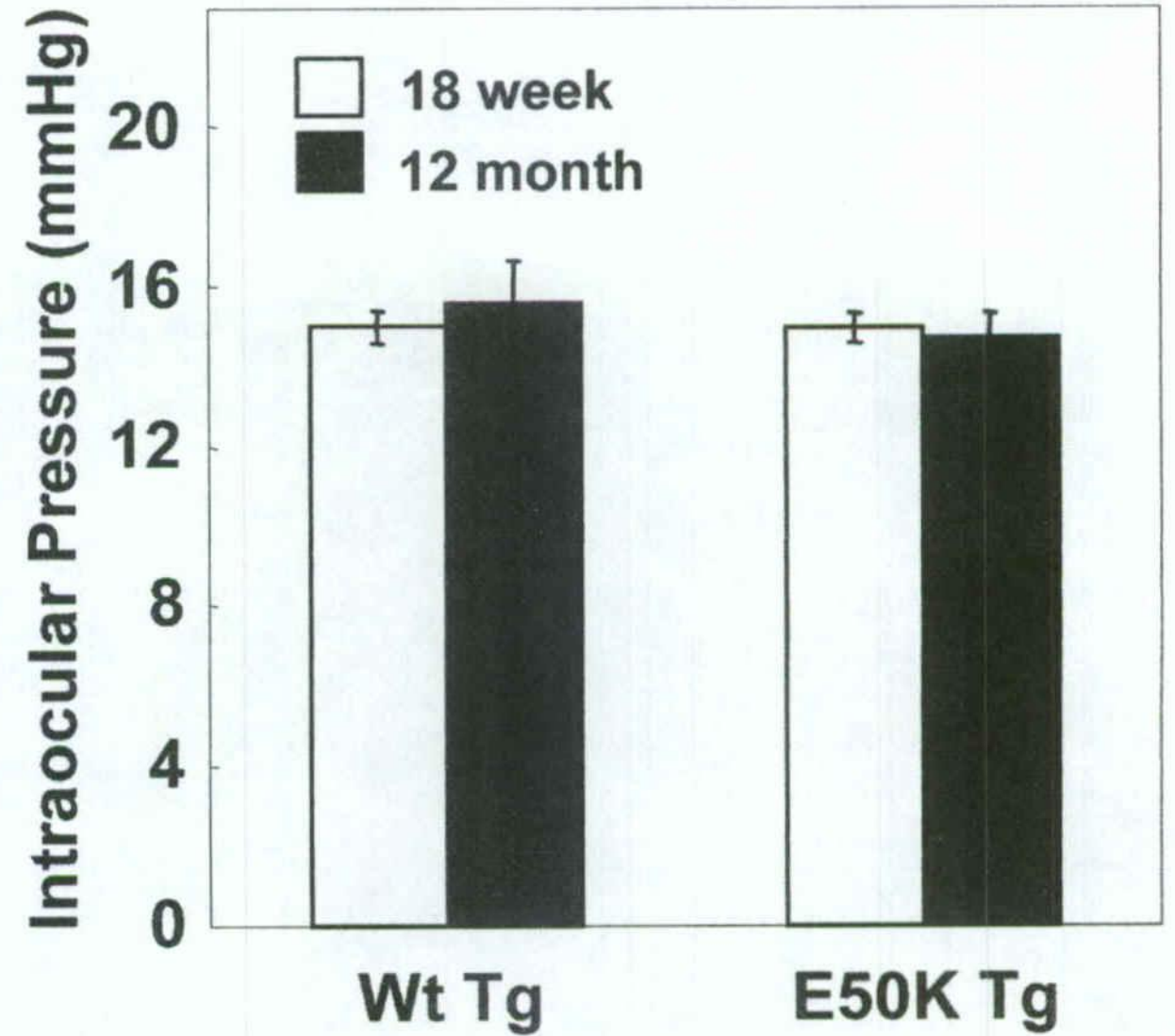
Merge

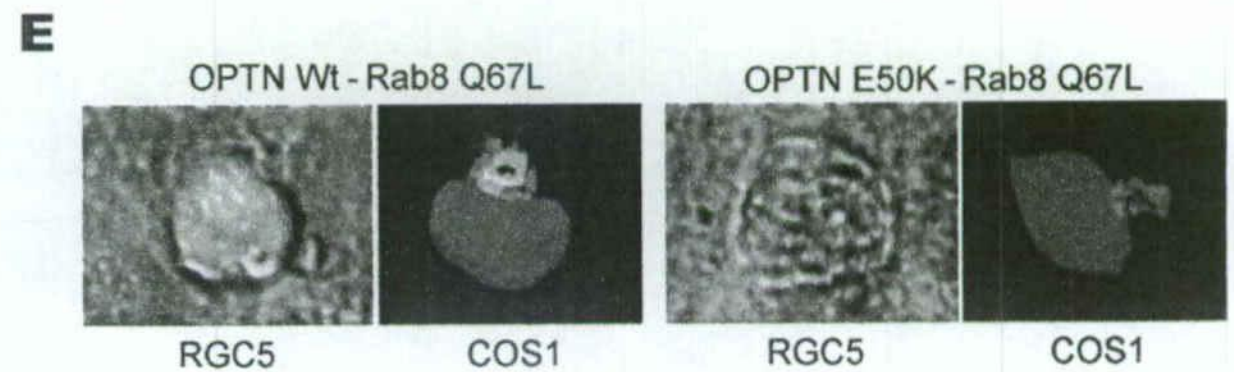
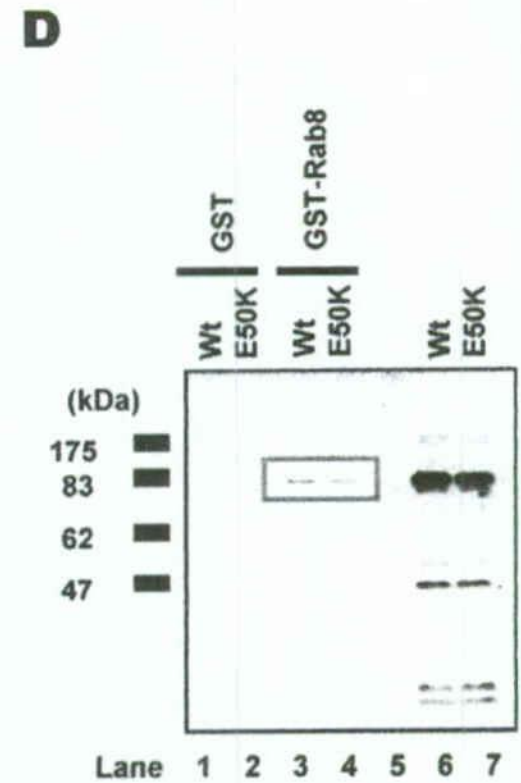
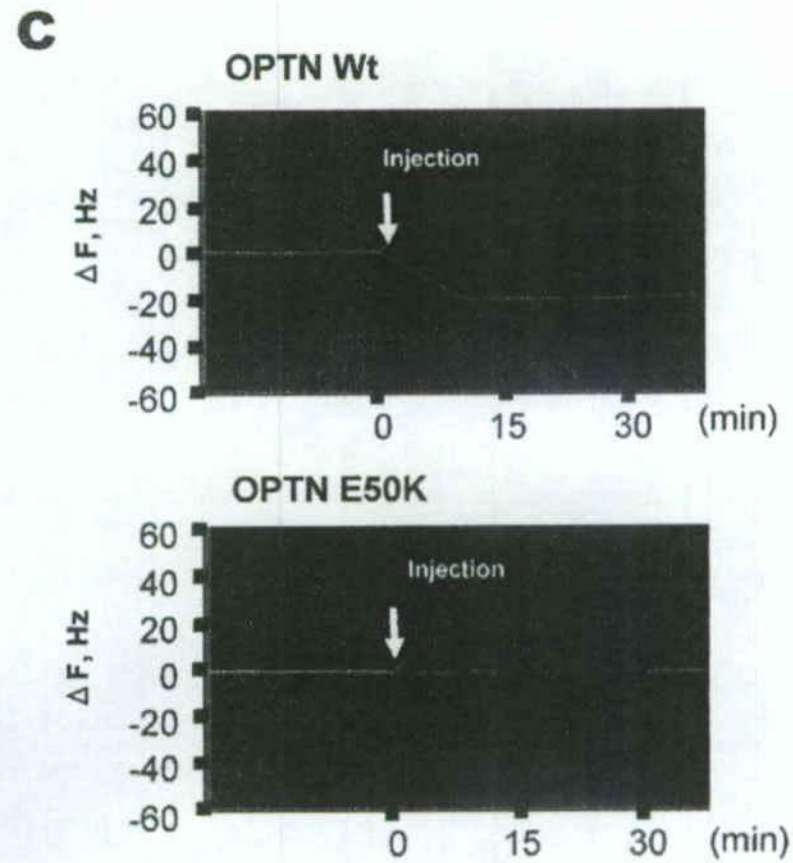
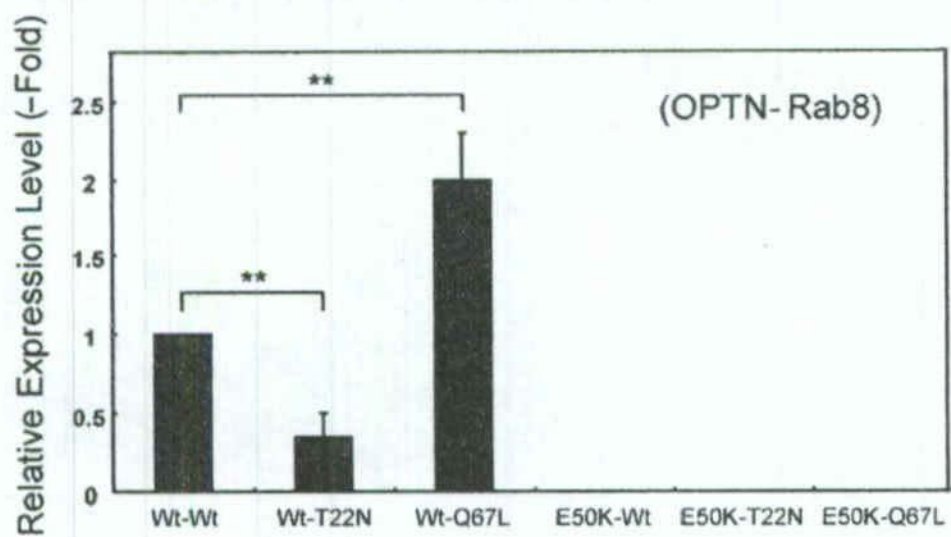
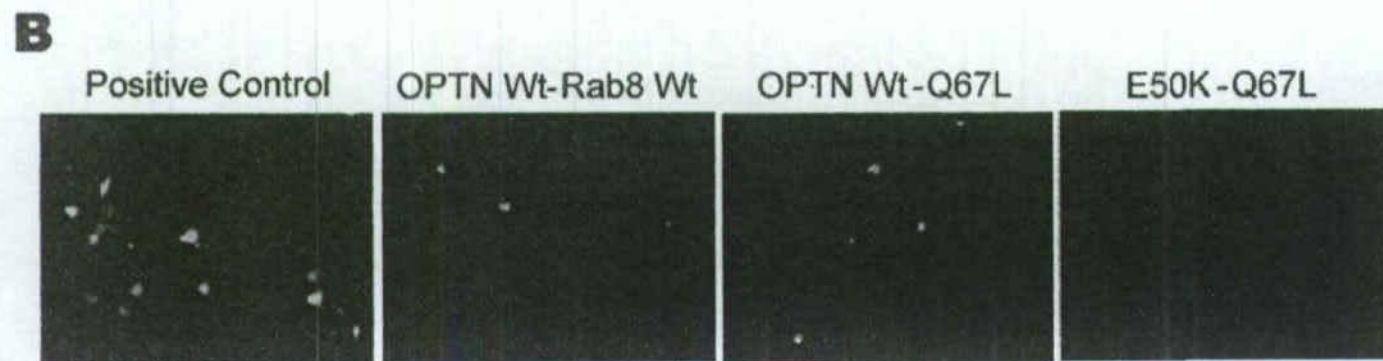
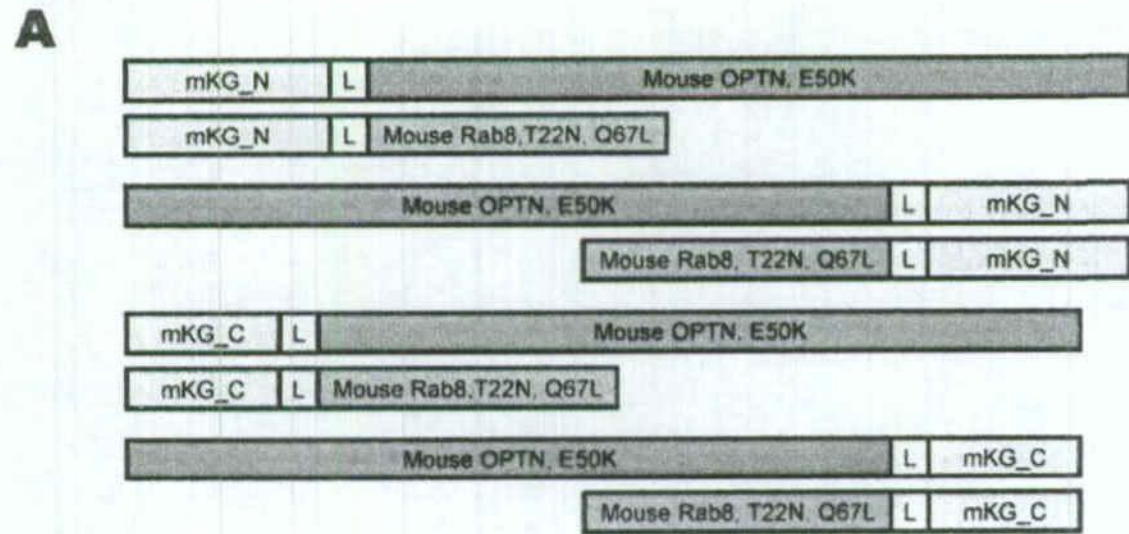


Peripheral

Central



A**Impact Rebound Tonometer****B****Optical Interferometry Tonometer**

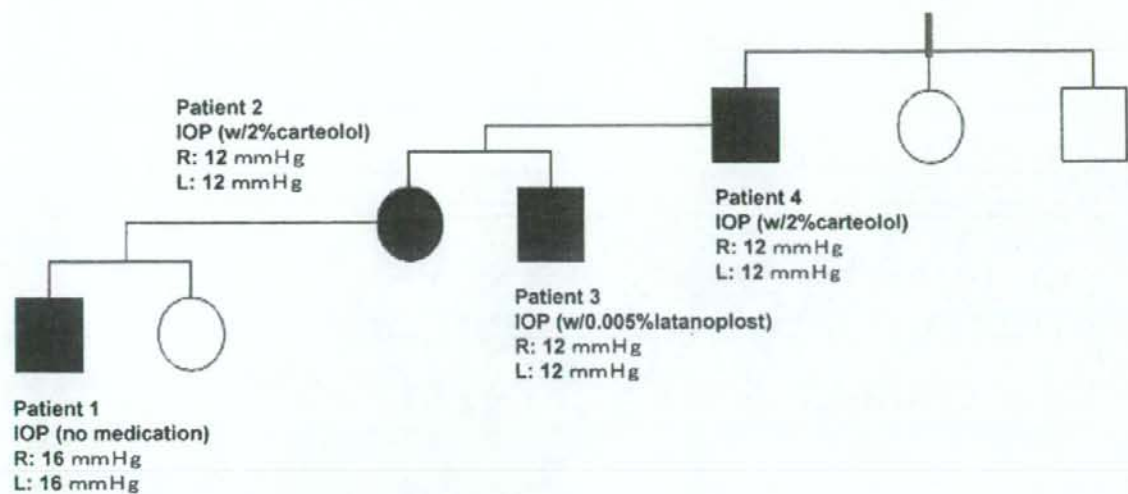
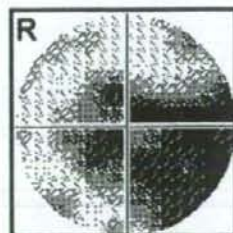
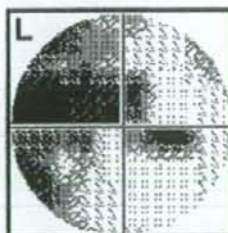
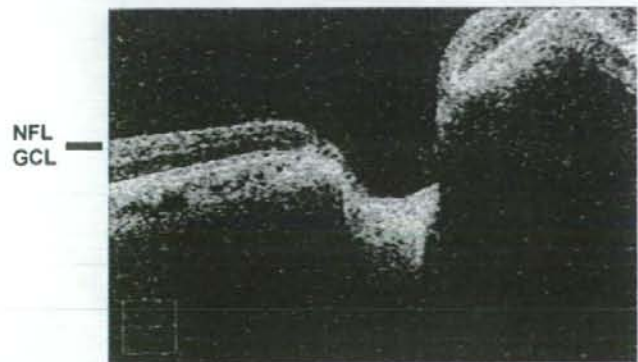


A

I

II

III

**B****Normal****Patient 2**

High Resolution Genome-wide Association Study
on Advanced Wet-type Age-Related Macular Degeneration

Asako Seki^{1*}, Masakazu Akahori^{1*}, Haru Okamoto¹, Masayoshi Minami¹, Naoki Terauchi²,
Minoru Obazawa², Tohru Noda², Miki Honda³, Atsushi Mizota³, Minoru Tanaka³, Takeshi
Iwata¹

*These two authors contributed equally to this manuscript

¹National Institute of Sensory Organs, National Hospital Organization Tokyo Medical Center, Meguro-ku, Tokyo, Japan. ²Division of Ophthalmology, National Hospital Organization Tokyo Medical Center, Meguro-ku, Tokyo, Japan. ³Department of Ophthalmology, Juntendo University Urayasu Hospital, Urayasu, Chiba, Japan.

Correspondence to: Takeshi Iwata, Ph.D.

Division of Molecular & Cellular Biology, National Institute of Sensory Organs, National Hospital Organization Tokyo Medical Center, 2-5-1 Higashigaoka, Meguro-ku, Tokyo 152-8902 Japan.

TEL/FAX: +81-3-34111026

Email: iwatatakeshi@kankakuki.go.jp

Word count:

Abstract

Age-related macular degeneration (AMD) is a multifactorial disease which affects mainly the central vision of the elderly population worldwide. The genetic contributions to the development of this disease have been extensively analyzed in various ethnic groups, and several susceptibility genes, e.g., complement factor H (*CFH*), *LOC387715*, and high temperature required A1 (*HTRA1*), have been identified. The latter two genes have been shown to be associated with all types of AMD, viz., geographic atrophy (dry-type), choroidal neovascularization (CNV, wet-type), and polypoidal choroidal vasculopathy (PCV-type). However, the mechanisms of how these genes participate in the onset of such different types of AMD are not well understood. Because many of the previous genome-wide association studies (GWAS) have included both the dry-type and wet-type of AMD, the genetic factors participating in a particular type of AMD may have been overlooked.

A higher resolution GWAS using Affymetrix 500K array set was conducted on selected Japanese patients with only the advanced form of wet-type AMD, to identify the genes that which may lead to the severe wet-type AMD. A case-control study was performed on 100 advanced wet-type AMD and 200 controls. Only the *LOC387715/HTRA1* region on chromosome 10 was significantly associated with the

advanced wet-type AMD in the Japanese. The *CFH* region on chromosome 1 was not associated with the wet-type AMD. The *P* values of rs10490924, rs3750848 and rs2672587 in this region were 1.19×10^{-13} , 1.38×10^{-13} , and 8.02×10^{-9} respectively. We conclude that the *LOC387715/HTRA1* region is a unique locus that is strongly associated with the advanced wet-type AMD in Japanese.

Key words: age-related macular degeneration, genome wide association study,

LOC387715, HTRA1

Introduction

AMD is a complex, multifactorial disease which is the main cause of irreversible decrease in vision in individuals over 65-years-of-age [??worldwide??] in western countries. The number of patients who are identified with AMD has been continuously increasing in Japan. AMD is a progressive disease with a wide spectrum of clinical findings that primarily affects the macular area of the retina.[1] The treatment of AMD has been primarily focused on the final stages of the disease, and consists of inhibiting the choroidal neovascularization (CNV) by antibodies against vascular endothelial growth factor (VEGF) or aptamer.[2] The results of recent studies have provided evidence that the risk factors for AMD are; genetics, behavioral, nutritional, and environmental factors.[1]

In Caucasians, early AMD is manifested by an increase in the number of large soft drusen, and the disease processes progresses to either the dry-type or wet-type AMD.[1] Recent studies have shown that both adaptive and innate immunological responses are activated around the retinal pigment epithelial (RPE) cells leaving traces of macrophages and activated complement factors in the drusen debris.[3]

In contrast to Caucasians with a high prevalence of the dry-type AMD with drusen, Japanese patients are predominantly affected with the wet-type AMD with CNVs and few